

A Systematic Exploration of Nickel–Pyrazolinato Chemistry with Alkali Metals: New Cages From Serendipitous Assembly

Guillem Aromí,^{*[a]} Aidan R. Bell,^[a] Madeleine Helliwell,^[a] James Raftery,^[a] Simon J. Teat,^[b] Grigore A. Timco,^[c] Olivier Roubeau,^[d] and Richard E. P. Winpenny^{*[a]}

Abstract: The preparation and properties of fourteen novel paramagnetic $[\text{Ni}^{\text{II}}_x]$ aggregates bridged by pivalate, pyrazolinolate and in most cases hydroxide are reported. A rich structural diversity has been achieved by changing the nature of the alkali of the base used during the synthesis, leading to the nuclearities $[\text{Ni}^{\text{II}}_4\text{Na}^{\text{I}}_4]$ (**2**, **3**, **4**), $[\text{Ni}^{\text{II}}_5\text{Na}^{\text{I}}_4]$ (**5**, **6**, **7**), $[\text{Ni}^{\text{II}}_5\text{Li}^{\text{I}}_6]$ (**8**), $[\text{Ni}^{\text{II}}_8\text{M}^{\text{I}}_2]$ ($\text{M} = \text{K}$ (**9**, **10**), Rb (**11**, **12**), Cs (**13**, **14**) and $[\text{Ni}^{\text{II}}_8]$ (**15**). All compounds have been characterised by single-crystal X-ray diffraction; however, full crystallographic details are given only for the representative molecules $[\text{Ni}_4\text{Na}_4(\text{fpo})_4(\text{piv})_8(\text{Hpiv})_8]$ (**2**), $[\text{Ni}_5\text{Na}_4(\text{OH})_2(\text{mpo})_4(\text{piv})_8(\text{Hpiv})_2(\text{MeCN})_2]$ (**5**),

$[\text{Ni}_5\text{Li}_6(\text{OH})_2(\text{fpo})_2(\text{piv})_{12}(\text{Hpiv})_4]$ (**8**), $[\text{Ni}_8\text{K}_2(\text{OH})_4(\text{ppo})_4(\text{piv})_{10}(\text{Hppo})_2(\text{Hpiv})_2(\text{MeCN})_2]$ (**9**), $[\text{Ni}_8\text{Rb}_2(\text{OH})_4(\text{ppo})_4(\text{piv})_{10}(\text{Hppo})_2(\text{Hpiv})_2(\text{MeCN})_2]$ (**11**), $[\text{Ni}_8\text{Cs}_2(\text{OH})_4(\text{ppo})_4(\text{piv})_{10}(\text{Hppo})_2(\text{Hpiv})_2(\text{MeCN})_2]$ (**13**) and $[\text{Ni}_8(\text{OH})_4(\text{mpo})_2(\text{PhCH}_2\text{CO}_2)_{10}(\text{Hmpo})_8]$ (**15**). Variable-temperature bulk magnetisation measurements have been performed for each type of complex. The $[\text{Ni}^{\text{II}}_4\text{Na}^{\text{I}}_4]$ clusters show intramolecular antiferromagnetic coupling and a spin ground state of $S = 0$. Complexes of the

type $[\text{Ni}^{\text{II}}_5\text{Na}^{\text{I}}_4]$ also display antiferromagnetic superexchange, leading to an $S = 1$ spin ground state. The molecule with nuclearity $[\text{Ni}^{\text{II}}_5\text{Li}^{\text{I}}_6]$, in contrast, exhibits ferromagnetic interactions, resulting in the presence of low energy states with high multiplicity, and a spin ground state $S > 1$. The $[\text{Ni}^{\text{II}}_8\text{M}^{\text{I}}_2]$ and $[\text{Ni}^{\text{II}}_8]$ clusters have the same topology of spin carriers, which display predominantly antiferromagnetic interactions to yield a diamagnetic ground state. The coupling within these octanuclear Ni^{II} clusters is rationalised in terms of the nature of the Ni–O–Ni angles within the core.

Keywords: alkali metals • cluster compounds • magnetic properties • nickel • serendipitous assembly

Introduction

All polymetallic compounds are made from complex reaction systems, which provide metal ions, ligand or ligands, solvent molecules, counter-ions and, perhaps, traces of moisture or absorbed oxygen. Each component may influence the final product. Other variables include the pH and ionic strength of the solution, and the temperature of the reaction. One route to polymetallic compounds—a route perhaps best termed “designed assembly”—controls the reaction pathway by

making a specific metal–ligand interaction the most significant in the system. Typical examples of this approach are the grids made by Lehn and co-workers,^[1,2] the sophisticated structures made by the Saalfrank group^[3,4] or the polyhedra constructed by Fujita and co-workers based on the concept of “molecular panelling”.^[5]

A complementary strategy is “serendipitous assembly”,^[6] where the variables in the complex system are modified following certain rationales to influence the product found, rather than to control or design the target molecule. The most extraordinary products from this route are the molybdate cages produced by Müller and co-workers,^[7,8] where an intuitive understanding of the reaction involved allows many magnificent structures to be prepared by subtle and rational variation in reaction conditions. Here we report some experiments in serendipitous assembly that lead to a new and diverse family of polymetallic nickel cages.

Results and Discussion

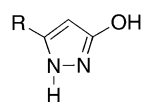
Synthesis and Crystal Structures: The original aim of this synthetic program was to explore the versatile bridging

[a] Dr. G. Aromí, Prof. R. E. P. Winpenny, A. R. Bell, Dr. M. Helliwell, Dr. J. Raftery
Department of Chemistry, The University of Manchester
Oxford Road, Manchester, M13 9PL (UK)
Fax: (+44)161-275-4616
E-mail: richard.winpenny@man.ac.uk

[b] Dr. S. J. Teat
CCLRC Daresbury Laboratory, Warrington
Cheshire, WA4 4AD (UK)

[c] Dr. G. A. Timco
Institute of Chemistry, Moldovan Academy of Sciences
Chişinău (Moldova)

[d] Dr. O. Roubeau
Centre de Recherche Paul Pascal
115 avenue du Dr Schweitzer, 33600 Pessac (France)



R = Me, Hmpo
R = Et, Hepo
R = CF₃, Hfpo
R = Ph, Hppo

potential of pyrazolinol-type ligands for the assembly of Ni^{II} ions into aggregates with novel structures and magnetic properties. It was observed that the complexes obtained incorporated the alkali metal of the base used initially to deprotonate

the ligands, and that their structure was sensitive to the nature of this alkali. Therefore, a systematic study was undertaken. A list of all the compounds presented in this report is given in Table 1. Full crystallographic details are given in Table 2 for one representative example of each structural type.

Table 1. List of the various complexes presented in this work.

[Ni ₂ (H ₂ O)(piv) ₄ (Hpiv) ₄]	(1)
[Ni ₄ Na ₄ (fpo) ₄ (piv) ₈ (Hpiv) ₈]	(2)
[Ni ₄ Na ₄ (mpo) ₄ (piv) ₈ (Hpiv) ₆]	(3)
[Ni ₄ Na ₄ (epo) ₄ (piv) ₈ (Hpiv) ₅]	(4)
[Ni ₅ Na ₄ (OH) ₂ (mpo) ₄ (piv) ₈ (Hpiv) ₂ (MeCN) ₂]	(5)
[Ni ₅ Na ₄ (OH) ₂ (epo) ₄ (piv) ₈ (MeCN) ₄]	(6)
[Ni ₅ Na ₄ (OH) ₂ (ppo) ₄ (piv) ₈ (Hpiv) ₂ (EtOAc) ₂]	(7)
[Ni ₅ Li ₆ (OH) ₂ (fpo) ₂ (piv) ₁₂ (Hpiv) ₄]	(8)
[Ni ₈ K ₂ (OH) ₄ (ppo) ₄ (piv) ₁₀ (Hppo) ₂ (Hpiv) ₂ (MeCN) ₂]	(9)
[Ni ₈ K ₂ (OH) ₄ (epo) ₄ (piv) ₁₀ (Hepo) ₄ (MeCN) ₂]	(10)
[Ni ₈ Rb ₂ (OH) ₄ (ppo) ₄ (piv) ₁₀ (Hppo) ₂ (Hpiv) ₂ (MeCN) ₂]	(11)
[Ni ₈ Rb ₂ (OH) ₄ (epo) ₄ (piv) ₁₀ (Hepo) ₄ (MeCN) ₂]	(12)
[Ni ₈ Cs ₂ (OH) ₄ (ppo) ₄ (piv) ₁₀ (Hppo) ₂ (Hpiv) ₂ (MeCN) ₂]	(13)
[Ni ₈ Cs ₂ (OH) ₄ (epo) ₄ (piv) ₁₀ (Hepo) ₂ (Hpiv) ₂ (MeCN) ₂]	(14)
[Ni ₈ (OH) ₄ (mpo) ₂ (PhCH ₂ CO ₂) ₁₀ (Hmpo) ₈]	(15)

Reactions with Na^I: The reaction of the sodium salt of various derivatives of pyrazolinol (R = Me, Hmpo; Et, Hepo; Ph, Hppo; CF₃, Hfpo) with the dinuclear Ni^{II} carboxylate [Ni₂(H₂O)(piv)₄(Hpiv)₄] (**1**)^[9] (Hpiv = trimethylacetic acid) was first investigated. A solution of the fluorinated ligand

Hfpo, sodium methoxide and complex **1** (0.63:1:1) in MeOH was stirred and evaporated to dryness. Extraction with MeCN led to the crystallisation of the mixed-metal cluster [Ni₄Na₄(fpo)₄(piv)₈(Hpiv)₈] (**2**) in good yield, as revealed by X-ray diffraction studies.

The molecular structure of **2** (Figure 1) shows a central core of four crystallographically equivalent Ni^{II} centres linked by four bridging fpo⁻ ligands. Each of the latter binds to one Ni ion through its α-N donor, and to two more Ni centres via the O atom, which in turn forms an additional bond with an

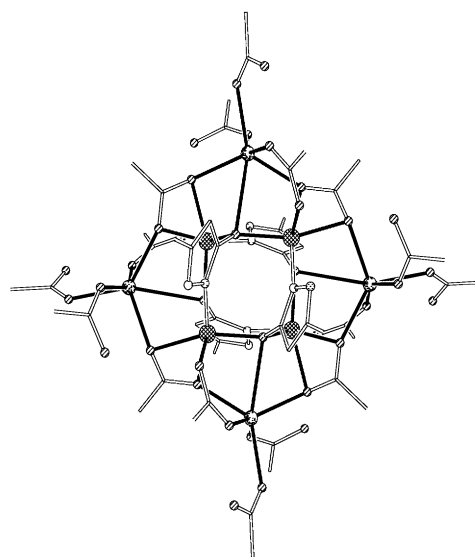


Figure 1. The structure of [Ni₄Na₄(fpo)₄(piv)₈(Hpiv)₈] (**2**) in the crystal. The hydrogen and fluorine atoms and the CH₃ groups from piv⁻ have been omitted for clarity. Code for atoms: large cross-hatched, Ni; medium heavy shadow dotted, Na; small shaded diagonal, O; small dotted, N; rest, C. Bond length ranges [Å]: Ni–O(fpo) 2.036–2.053, Ni–N(fpo) 2.032, Ni–O(piv) 2.043–2.205, Na–O(fpo) 2.869, Na–O(piv) 2.296–2.385, Na–O(Hpiv) 2.367–2.373.

Table 2. Crystallographic data for compounds [Ni₄Na₄(fpo)₄(piv)₈(Hpiv)₈](**2**), [Ni₅Na₄(OH)₂(mpo)₄(piv)₈(Hpiv)₂(MeCN)₂](**5**), [Ni₅Li₆(OH)₂(fpo)₂(piv)₁₂(Hpiv)₄](**8**) [Ni₈K₂(OH)₄(ppo)₄(piv)₁₀(Hppo)₂(Hpiv)₂(MeCN)₂](**9**), [Ni₈Rb₂(OH)₄(ppo)₄(piv)₁₀(Hppo)₂(Hpiv)₂(MeCN)₂](**11**), [Ni₈Cs₂(OH)₄(ppo)₄(piv)₁₀(Hppo)₂(Hpiv)₂(MeCN)₂](**13**), [Ni₈(OH)₄(mpo)₂(PhCH₂CO₂)₁₀(Hmpo)₈](**15**).

	2	5	8	9	11	13	15
dimensions [mm]	0.35 × 0.08 × 0.08	0.60 × 0.50 × 0.50	0.30 × 0.30 × 0.10	0.40 × 0.40 × 0.30	0.50 × 0.30 × 0.01	0.40 × 0.15 × 0.10	0.08 × 0.07 × 0.02
system	tetragonal	monoclinic	triclinic	monoclinic	monoclinic	triclinic	triclinic
group	<i>I</i> $\bar{4}$	<i>P</i> 2(1)/ <i>n</i>	<i>P</i> $\bar{1}$	<i>C</i> 2/ <i>c</i>	<i>C</i> 2/ <i>c</i>	<i>P</i> $\bar{1}$	<i>P</i> $\bar{1}$
<i>a</i> [Å]	21.1635(17)	18.6063(15)	14.040(2)	35.623(3)	35.679(4)	15.8882(13)	18.9422(13)
<i>b</i> [Å]	21.1635(17)	14.1457(11)	16.253(3)	15.9901(14)	15.9236(16)	18.7314(16)	19.6604(13)
<i>c</i> [Å]	14.3052(16)	19.8011(15)	16.337(3)	28.042(2)	28.083(3)	26.781(2)	19.8493(13)
α [°]	90.00	90.00	62.805(2)	90.00	90.00	74.083(2)	89.921(2)
β [°]	90.00	116.7580(10)	64.620(2)	112.487(2)	112.452(2)	81.108(2)	78.874(2)
γ [°]	90.00	90.00	66.520(2)	90.00	90.00	73.670(2)	89.978(2)
<i>V</i> [Å ³]	6407.2(10)	4653.5(6)	2899.1(8)	14759(2)	14745(3)	7329.4(11)	7253.2(8)
<i>Z</i>	2	2	2	4	8	2	2
ρ_{calcd} [g cm ⁻³]	1.325	1.357	1.301	1.308	1.334	1.458	1.461
$2\theta_{\text{max}}$	52.8	52.88	52.74	57.08	52.74	52.78	50.00
radiation	MoK α	MoK α	MoK α	MoK α	MoK α	MoK α	synchrotron
λ [Å]	0.71073	0.71073	0.71073	0.71073	0.71073	0.71073	0.6869
<i>T</i> [K]	100	100	100	100	100	100	150
reflns	18679	26347	23103	45643	58181	42499	52780
ind. reflns	6512	9543	11662	17165	15078	29126	38339
reflns with <i>I</i> > 2 σ (<i>I</i>)	5948	8430	8522	12256	10422	23093	25383
<i>R</i> 1	0.0368	0.0353	0.0658	0.1002	0.1081	0.0544	0.0969
<i>wR</i> 2	0.0615	0.0785	0.1193	0.2244	0.2228	0.0859	0.1631

external Na^I metal (4.31 coordination mode using Harris notation^[10]). The Ni centres are disposed in a flattened tetrahedral architecture, with the four equivalent edges capped by one Na cation to form a [Ni₄Na₄] cage. Eight additional pivalate ligands also bridge between Na and Ni, in a 2.11 or a 3.22 bridging mode. The sixfold coordination around each Na^I is completed by two monodentate Hpiv molecules. The coordination sphere around Ni^{II} is distorted octahedral, with an "O₅N" donor set. The same reaction performed with Hmpo and Hepo led to the isolation of the analogous complexes [Ni₄Na₄(mpo)₄(piv)₈(Hpiv)₆] (**3**) and [Ni₄Na₄(epo)₄(piv)₈(Hpiv)₅] (**4**), respectively, as determined by X-ray crystallography. Complexes **3** and **4** possess two and three less terminal Hpiv ligands, respectively, than **2**; this results in the presence of two and three pentacoordinate Na^I ions, respectively. This difference persists in the bulk material, as corroborated by elemental analyses (see Experimental Section).

The presence of five to eight terminal pivalic acid ligands in these [Ni₄Na₄] cages suggested that use of more base during the reaction could lead to deprotonation of these ligands and to a structural change. Indeed, when the synthesis involving **1**/Hmpo/NaOMe was repeated, but with 1:2:4 stoichiometry (instead of 0.63:1:1), green crystals of a new complex could be obtained from the MeCN extract and were identified as the heterometallic species [Ni₅Na₄(OH)₂(mpo)₄(piv)₈(Hpiv)₂(MeCN)₂] (**5**).

This molecule has a much lower content of Hpiv than **2–4**, and its structure (Figure 2) shows a completely different topological arrangement. Complex **5** features a core of five Ni^{II} ions disposed in a centred parallelogram, which is planar

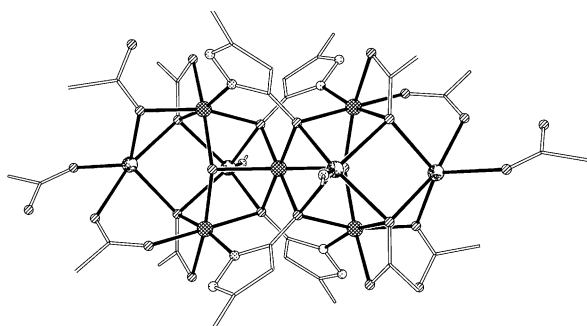


Figure 2. The structure of [Ni₅Na₄(OH)₂(mpo)₄(piv)₈(Hpiv)₂(MeCN)₂] (**5**) in the crystal. The hydrogen atoms and the CH₃ groups from piv⁻ have been omitted for clarity. Code for atoms: large cross-hatched, Ni; medium heavy shadow dotted, Na; small shaded diagonal, O; small dotted, N; rest, C. Bond length ranges [Å]: Ni–O(mpo) 2.053–2.105, Ni–N(mpo) 2.020–2.024, Ni–O(OH) 2.047–2.107, Ni–O(piv) 2.080–2.220, Na–O(mpo) 2.370–2.396, Na–O(piv) 2.290–2.439, Na–O(Hpiv) 2.356, Na–N(MeCN) 2.400.

by virtue of a crystallographic inversion centre. As in the above family of compounds, the four mpo⁻ ligands bridge between the Ni centres; the mpo⁻ ligands display the same coordination mode as before (4.31), therefore, each of them forms a further bond to Na^I through the O donor. In **5** however, two additional μ₃-OH⁻ ligands contribute to the cementing of the central [Ni₅] unit. Pivalate ligands ensure, partially or exclusively, the binding of a total of four Na^I ions

to the central metallic core, capping both short edges of the Ni parallelogram. The piv⁻ ligands are found in the 2.11, 2.20 or 3.31 bridging modes. The square pyramidal coordination around Na^I is completed by either MeCN or Hpiv terminal ligands, the latter forming hydrogen bonds with the oxygen of two neighbouring μ-piv⁻ groups. The coordination geometry around all Ni centres is distorted octahedral. When the same reaction was performed with Hepo, a complex very similar to **5** was obtained, namely [Ni₅Na₄(OH)₂(epo)₄(piv)₈(MeCN)₄] (**6**), in which MeCN takes the positions occupied by Hpiv in complex **5**. The analogous complex [Ni₅Na₄(OH)₂(ppo)₄(piv)₈(Hpiv)₂(EtOAc)₂] (**7**) was prepared with the phenyl derivative Hppo, thereby confirming the [Ni₅Na₄] structural unit as a recurrent arrangement under this set of conditions. Use of ethyl acetate as the extracting solvent instead of MeCN explains the presence of two EtOAc molecules as terminal ligands.

Reactions with Li^I: The observation that in both of the structural types unveiled above Na^I was contained as an integral part of the cluster led to the thought that the topology of the resulting product could be controlled by the nature of the alkali metal employed. Thus, the reactivity that gave place to complexes **2** to **7** was explored by using LiOMe as the source of base. From the reaction of **1**, Hfpo and LiOMe (1:2:2) in MeOH the new complex [Ni₅Li₆(OH)₂(fpo)₂(piv)₁₂(Hpiv)₄] (**8**) was isolated, as shown by single-crystal X-ray diffraction studies. The structure of **8** (Figure 3) is reminiscent of that of complexes **5**, **6** and **7**, in that it has a central core of five Ni^{II} centres disposed in a centred parallelogram featuring an inversion centre in the middle. Complex **8**, however, features a total of six alkali metals (Li^I) as a part of the cluster and a number of ligands and bridging modes different from those in the above [Ni₅] complexes. In this case, the bridging between the Ni^{II} ions is carried out by two fpo⁻ ligands, two μ₃-OH⁻ groups and four pivalate donors. As in **2** to **7**, two Ni^{II} ions participate in the 4.31 coordination

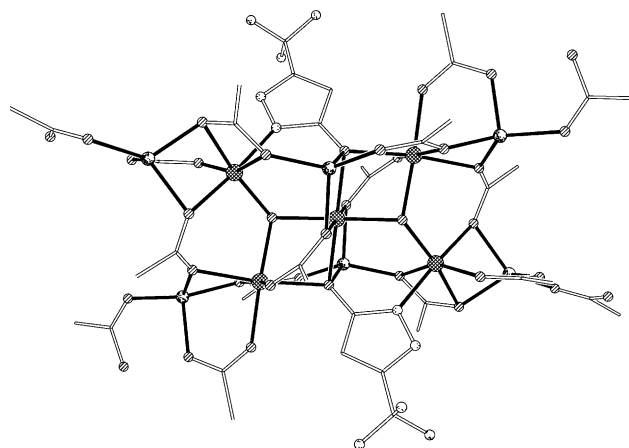


Figure 3. The structure of [Ni₅Li₆(OH)₂(fpo)₂(piv)₁₂(Hpiv)₄] (**8**) in the crystal. The hydrogen atoms and the CH₃ groups from piv⁻ have been omitted for clarity. Code for atoms: large cross-hatched, Ni; medium heavy shadow dotted, Li; small shaded diagonal, O; small dotted, N and F; rest, C. Bond length ranges [Å]: Ni–O(fpo) 2.138–2.146, Ni–N(fpo) 2.033, Ni–O(piv) 2.034–2.197, Li–O(fpo) 1.998, Li–O(piv) 1.809–2.044, Na–O(Hpiv) 1.936–1.949.

mode of the ppo^- moieties, in addition to one alkali ion, which is connected to the ligand through the O atom. The six Li^+ ions cap both long sides and the four vertices of the parallelogram, and are connected to Ni through the ppo^- groups and a total of twelve pivalate ligands, which are found in a variety of bridging modes: 2.11, 3.21, 3.22 and 4.22. The coordination geometry around Li^+ is distorted tetrahedral and is completed by one molecule of pivalic acid, while the Ni^{II} centres display distorted octahedral environment.

Reactions with K^+ , Rb^+ and Cs^+ : The above results showed that changing the nature of the alkali metal in the reaction system was a way of introducing dramatic structural changes to the final product. This prompted the investigation of the corresponding experiments with K^+ , Rb^+ and Cs^+ . Reactions involving KOEt, with ligands Hppo or Hepo led to the new heterometallic complexes $[\text{Ni}_8\text{K}_2(\text{OH})_4(\text{ppo})_4(\text{piv})_{10}(\text{Hppo})_2(\text{Hpiv})_2(\text{MeCN})_2]$ (**9**) and $[\text{Ni}_8\text{K}_2(\text{OH})_4(\text{epo})_4(\text{piv})_{10}(\text{Hepo})_4(\text{MeCN})_2]$ (**10**), respectively, as determined crystallographically, irrespective of the various stoichiometries used.

The X-ray structures of **9** (Figure 4) and **10** show that the cation K^+ supports a completely different architecture from those of Li^+ and Na^+ . Complex **9** features a core composed of

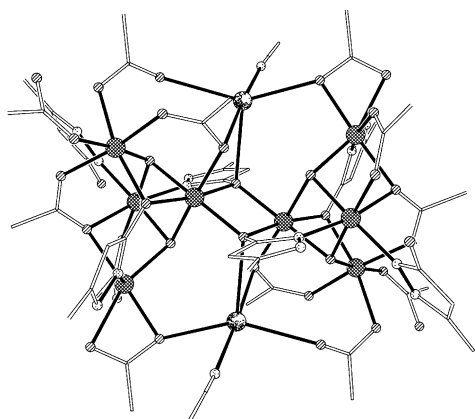


Figure 4. The structure in the crystal of $[\text{Ni}_8\text{K}_2(\text{OH})_4(\text{ppo})_4(\text{piv})_{10}(\text{Hppo})_2(\text{Hpiv})_2(\text{MeCN})_2]$ (**9**). The hydrogen atoms and the CH_3 groups from piv^- have been omitted for clarity. Code for atoms: large cross-hatched, Ni; large heavy shadow dotted, K; small shaded diagonal, O; small dotted, N; rest, C. Bond length ranges [\AA]: Ni–O(ppo) 2.047–2.117, Ni–N(ppo) 2.029–2.076, Ni–O(OH) 1.988–2.059, Ni–O(piv) 2.018–2.282, Ni–O(Hpiv) 2.075, K–O(ppo) 2.715, K–O(piv) 2.600–2.824, K–N(MeCN) 2.644.

two symmetrically related groups of four bridged Ni^{II} centres. Each of these $[\text{Ni}_4]$ units can be perceived as part of a $[\text{Ni}_4(\mu_3\text{-O})_2(\mu\text{-O})_2]$ pseudo cubane (Figure 6 below) with two missing edges. The $\mu_3\text{-O}$ atoms in this unit belong to OH^- groups, and the $\mu\text{-O}$ donors come from one carboxylate group and one ppo^- ligand in the 3.21 coordination mode. A direct link between these tetranuclear moieties is provided by the O-atoms of two equivalent ppo^- groups, which bridge from the Ni^{II} of one unit to its equivalent on the other. The coordination mode of these ligands is 4.31, with the $\alpha\text{-N}$ donor bound to a third Ni^{II} centre and the oxygen atom further bound to a K^+ cation. Ten bridging pivalate groups contribute to the linkage between the metals within the cluster in a rich

variety of coordination modes: 3.21, 2.21 and 2.11. Unlike the case of **2–8**, four of the Ni^{II} ions in this molecule possess a terminal ligand, more precisely, two Hppo and two Hpiv ligands. The pentacoordination around each K^+ centre is completed by one MeCN molecule. All the Ni^{II} centres are in a distorted octahedral environment. The structure of **10** shows that this complex is almost exactly the Hepo analogue of **9**, with the exception that the Hpiv terminal ligands have been replaced by Hepo groups.

Experiments involving the next members (Rb and Cs) in the series of alkali metals were stimulated by the prospect of enlarging the rich structural diversity observed with Li, Na and K. The reaction between complex **1** and Hppo or Hepo was performed exactly as for **9** or **10**, respectively, by using RbOH in place of KOEt. As a result, crystals of complexes $[\text{Ni}_8\text{Rb}_2(\text{OH})_4(\text{ppo})_4(\text{piv})_{10}(\text{Hppo})_2(\text{Hpiv})_2(\text{MeCN})_2]$ (**11**) and $[\text{Ni}_8\text{Rb}_2(\text{OH})_4(\text{epo})_4(\text{piv})_{10}(\text{Hepo})_4(\text{MeCN})_2]$ (**12**) were obtained, which were suitable for X-ray crystallography. The above reactions were also conducted with $\text{Cs}(\text{OH})$ to produce the complexes $[\text{Ni}_8\text{Cs}_2(\text{OH})_4(\text{ppo})_4(\text{piv})_{10}(\text{Hppo})_2(\text{Hpiv})_2(\text{MeCN})_2]$ (**13**) and $[\text{Ni}_8\text{Cs}_2(\text{OH})_4(\text{epo})_4(\text{piv})_{10}(\text{Hepo})_2(\text{Hpiv})_2(\text{MeCN})_2]$ (**14**), respectively, as revealed by X-ray diffraction experiments. These again have the same metal core as **9** and **10**. A study is currently being undertaken in order to correlate the alkali cation size to the geometric parameters of the resulting clusters.

The above observations could lead to the conclusion that a large alkali cation (K^+ , Rb^+ or Cs^+) is necessary for the stabilisation of the $[\text{Ni}_8]$ core. This conclusion was contradicted by the results achieved from reactions involving a different carboxylate. Thus, stirring of a solution containing equimolar amounts of $\text{Ni}(\text{NO}_3)_2 \cdot 4\text{H}_2\text{O}$, $\text{Na}(\text{PhCH}_2\text{CO}_2)$ and $\text{Na}(\text{mpo})$ in MeOH gave a crude material after evaporation, which was extracted with EtOAc to slowly produce crystals of the new homometallic cage $[\text{Ni}_8(\text{OH})_4(\text{mpo})_2(\text{PhCH}_2\text{CO}_2)_{10}(\text{Hmpo})_8]$ (**15**). The X-ray molecular structure of this cluster (Figure 5) reveals a $[\text{Ni}_8\text{O}_{10}]$ core essentially identical

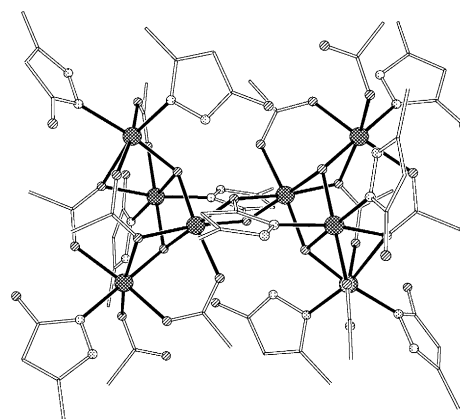


Figure 5. The structure in the crystal of $[\text{Ni}_8(\text{OH})_4(\text{mpo})_2(\text{PhCH}_2\text{CO}_2)_{10}(\text{Hmpo})_8]$ (**15**). The hydrogen atoms and the Ph rings from $\text{PhCH}_2\text{CO}_2^-$ have been omitted for clarity. Code for atoms: large cross-hatched, Ni; small shaded diagonal, O; small dotted, N; rest, C. Bond length ranges [\AA]: Ni–O(mpo) 2.051–2.128, Ni–N(ppo) 2.034–2.078, Ni–O(OH) 1.982–2.051, Ni–O(PhCH_2CO_2) 2.016–2.356, Ni–O($\text{PhCH}_2\text{CO}_2\text{H}$) 2.075.

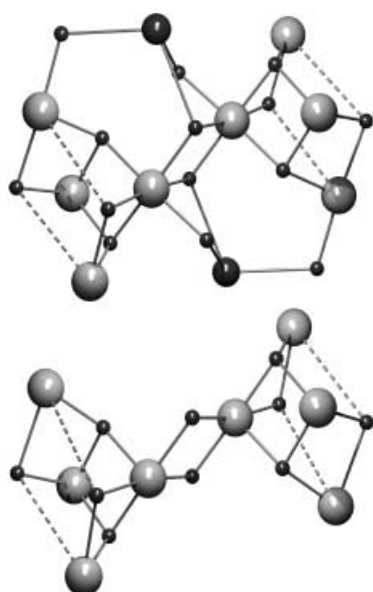


Figure 6. Comparison of the cores of complexes $[\text{Ni}_8\text{K}_2(\text{OH})_4(\text{ppo})_4(\text{piv})_{10}(\text{Hppo})_2(\text{Hpiv})_2(\text{MeCN})_2]$ (**9**) (top) and $[\text{Ni}_8(\text{OH})_4(\text{mpo})_2(\text{PhCH}_2\text{CO}_2)_{10}(\text{Hmpo})_8]$ (**15**) (bottom). Code for atoms: large, Ni; medium, K; small, O. The dashed lines are guides to the eye.

to the nickel core of complexes **9** to **14**. In Figure 6, a comparison between the core of **9** and that of **15** is shown.

In **15**, both μ -O atoms in each pseudo cubane originate from carboxylates. This complex only contains two deprotonated mpo^- ligands, which provide, as in the rest of the $[\text{Ni}_8]$ clusters, the central link between both groups of four Ni ions. Given the absence of an alkali metal, these mpo^- groups are in the coordination mode 3.21. In this molecule there are eight carboxylate groups acting as bridging ligands in modes equally distributed between 3.21 and 2.11. A total of eight Hmpo and two $\text{PhCH}_2\text{CO}_2^-$ groups complete the pseudo-octahedral environment around Ni^{II} as terminal ligands. Complex **15** does not incorporate Na^{I} into the structure because in this case the alkali metal remained behind as its solid nitrate salt when the crude product was extracted with EtOAc and filtered.

Magnetic Properties: Magnetic studies were carried out for complexes $[\text{Ni}_4\text{Na}_4(\text{epo})_4(\text{piv})_8(\text{Hpiv})_5]$ (**4**), $[\text{Ni}_5\text{Na}_4(\text{OH})_2(\text{ppo})_4(\text{piv})_8(\text{Hpiv})_2(\text{H}_2\text{O})_2]$ (**7a**), $[\text{Ni}_5\text{Li}_6(\text{OH})_2(\text{fpo})_2(\text{piv})_{12}(\text{Hpiv})_4]$ (**8**), $[\text{Ni}_8\text{K}_2(\text{OH})_4(\text{ppo})_4(\text{piv})_{10}(\text{Hppo})_2(\text{Hpiv})_2(\text{MeCN})_2]$ (**9**), $[\text{Ni}_8\text{Rb}_2(\text{OH})_4(\text{ppo})_4(\text{piv})_{10}(\text{Hppo})_2(\text{Hpiv})_2(\text{H}_2\text{O})_2]$ (**11a**), $[\text{Ni}_8\text{Cs}_2(\text{OH})_4(\text{ppo})_4(\text{piv})_{10}(\text{Hppo})_2(\text{Hpiv})_2(\text{MeCN})_2]$ (**13**) and $[\text{Ni}_8(\text{OH})_4(\text{mpo})_2(\text{PhCH}_2\text{CO}_2)_{10}(\text{Hmpo})_8]$ (**15**), as representative examples of the above family. Complexes **7a** and **11a** result from replacement of solvate ligands by H_2O molecules in compounds **7** and **11**, respectively. In all cases, bulk magnetic susceptibility measurements were performed on microcrystalline samples under a constant magnetic field of 1 kG (**4**, **7a**, **8**, **9**, **13** and **15**) or 10 kG (**11a**) in the 1.8–300 K temperature range.

$[\text{Ni}^{\text{II}}_4\text{Na}^{\text{I}}_4]$ complexes: The cage $[\text{Ni}_4\text{Na}_4(\text{epo})_4(\text{piv})_8(\text{Hpiv})_5]$ (**4**) was investigated as representative example of the group of $[\text{Ni}^{\text{II}}_4\text{Na}^{\text{I}}_4]$ complexes. The value of $\chi_m T$ (χ_m = magnetic

susceptibility) at 300 K was $5.61 \text{ cm}^3 \text{ K mol}^{-1}$, close to the value for four isolated Ni^{II} centres with octahedral geometry, $^3\text{A}_2$ ground state and $g = 2.2$, a common g value for this ion^[11] ($4.84 \text{ cm}^3 \text{ K mol}^{-1}$). The slight linear decrease of $\chi_m T$ as the temperature is decreased is probably due to a small, uncorrected diamagnetic contribution and/or to the existence of a small temperature-independent paramagnetism (TIP) factor. In the vicinity of 50 K, the decrease of $\chi_m T$ is distinctly sharper, reaching a value of $0.20 \text{ cm}^3 \text{ K mol}^{-1}$ at 1.8 K, caused by intramolecular antiferromagnetic interactions between Ni^{II} centres. The ground state is likely to be diamagnetic.

$[\text{Ni}^{\text{II}}_5\text{Na}^{\text{I}}_4]$ and $[\text{Ni}^{\text{II}}_5\text{Li}^{\text{I}}_6]$ complexes: The cluster $[\text{Ni}_5\text{Na}_4(\text{OH})_2(\text{ppo})_4(\text{piv})_8(\text{Hpiv})_2(\text{H}_2\text{O})_2]$ (**7a**) was chosen to represent the family of $[\text{Ni}^{\text{II}}_5\text{Na}^{\text{I}}_4]$ complexes, and its magnetic properties were compared with these of the compound $[\text{Ni}_5\text{Li}_6(\text{OH})_2(\text{fpo})_2(\text{piv})_{12}(\text{Hpiv})_4]$ (**8**), which has the same topology of Ni^{II} ions as the former but with different connectivity. Interestingly, the magnetic properties of these two types of pentanuclear Ni^{II} compounds were found to be in sharp contrast. This is shown in Figure 7, where plots of

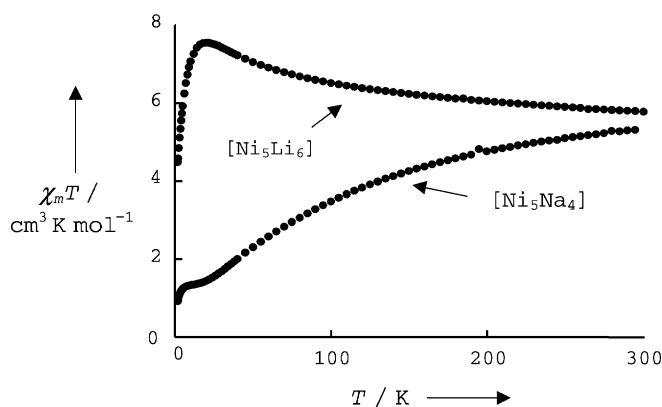


Figure 7. Plot of experimental $\chi_m T$ versus T for compounds $[\text{Ni}_5\text{Na}_4(\text{OH})_2(\text{ppo})_4(\text{piv})_8(\text{Hpiv})_2(\text{EtOAc})_2]$ (**7a**) and $[\text{Ni}_5\text{Li}_6(\text{OH})_2(\text{fpo})_2(\text{piv})_{12}(\text{Hpiv})_4]$ (**8**).

experimental $\chi_m T$ versus T for **7a** and **8**, are given. Both complexes display values of $\chi_m T$ at room temperature (5.38 and $5.77 \text{ cm}^3 \text{ K mol}^{-1}$ for **7a** and **8**, respectively) that are close to the expected value for five magnetically uncoupled $S = 1$ Ni^{II} centres with $g = 2.2$ (6.05). For complex **7a**, $\chi_m T$ starts to decrease with decreasing temperature even at room temperature until a plateau is reached at about $1.2 \text{ cm}^3 \text{ K mol}^{-1}$ and approximately 30 K. This shows the presence of strong antiferromagnetic interactions within the molecule, leading to a spin ground state of $S_T = 1$ (the expected spin-only value of $\chi_m T$ for an isolated triplet spin ground state with $g = 2.2$ is $1.21 \text{ cm}^3 \text{ K mol}^{-1}$). This assumption is supported by variable-field magnetisation measurements performed on a sample of complex **7a** at 1.8 K (not shown). The isothermal curve of reduced magnetisation saturates at about 2.2, very close to the expected value for an $S_T = 1$ ground state (2.2 for $g = 2.2$). This ground state can be understood in terms of two strongly antiferromagnetically coupled (diamagnetic) pairs to either side of the central Ni^{II} ion, which is responsible for the

remaining $S = 1$ spin ground state. In contrast to **7a**, the value of $\chi_m T$ for complex **8** (Figure 7) increases with decreasing temperature to attain a maximum of $7.55 \text{ cm}^3 \text{ K mol}^{-1}$ at 20 K, and then decreases sharply down to $4.48 \text{ cm}^3 \text{ K mol}^{-1}$ at 1.8 K. This is clearly indicative of the existence of ferromagnetic interactions within this cluster leading to either an $S_T > 1$ or to an $S_T = 1$ ground state with very low-lying excited states with high-spin multiplicity. Magnetisation measurements were also performed on complex **8**; however, the curves did not reach saturation and therefore the nature of the ground state could not be established. A detailed study of the magnetic properties of the $[\text{Ni}^{\text{II}}_5\text{Na}^{\text{I}}_4]$ and $[\text{Ni}^{\text{II}}_5\text{Li}^{\text{I}}_6]$ complexes is now underway to explain the important differences between them and to assess the exact nature of their spin ground states; this will be published elsewhere.

$[\text{Ni}^{\text{II}}_8\text{M}^{\text{I}}_2]$ ($\text{M} = \text{K}, \text{Rb}, \text{Cs}$) and $[\text{Ni}^{\text{II}}_8]$ clusters: Complexes $[\text{Ni}_8\text{K}_2(\text{OH})_4(\text{ppo})_4(\text{piv})_{10}(\text{Hppo})_2(\text{Hpiv})_2(\text{MeCN})_2]$ (**9**), $[\text{Ni}_8\text{Rb}_2(\text{OH})_4(\text{ppo})_4(\text{piv})_{10}(\text{Hppo})_2(\text{Hpiv})_2(\text{H}_2\text{O})_2]$ (**11a**), $[\text{Ni}_8\text{Cs}_2(\text{OH})_4(\text{ppo})_4(\text{piv})_{10}(\text{Hppo})_2(\text{Hpiv})_2(\text{MeCN})_2]$ (**13**) and $[\text{Ni}_8(\text{OH})_4(\text{mpo})_2(\text{PhCH}_2\text{CO}_2)_{10}(\text{Hmpo})_8]$ (**15**) were investigated to assess the magnetic properties within the octanuclear Ni^{II} core. In all cases the behaviour was very similar; this confirms that neither the nature of the alkali metal nor its absence had a profound effect on the magnetochemistry of this spin topology. In Figure 8 presents plots of $\chi_m T$ versus T and χ_m versus T for complex **9**, taken as an example for this

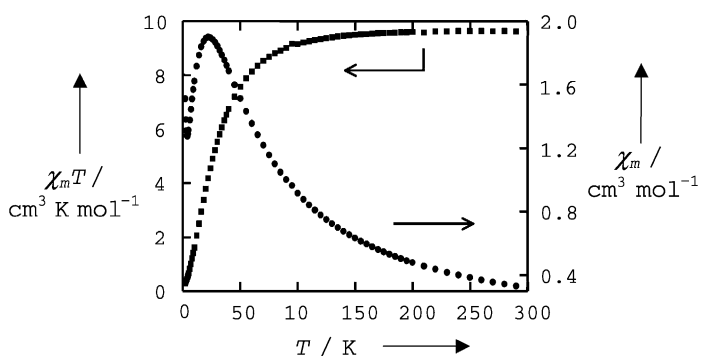


Figure 8. Plot of experimental $\chi_m T$ versus T (\bullet) and χ_m versus T (\blacksquare) for the complex $[\text{Ni}_8\text{K}_2(\text{OH})_4(\text{ppo})_4(\text{piv})_{10}(\text{Hppo})_2(\text{Hpiv})_2(\text{MeCN})_2]$ (**9**).

group of complexes. In all cases, the value of $\chi_m T$ at room temperature was similar to that expected for eight magnetically isolated Ni^{II} ($S = 1$) centres with $g = 2.2$ ($9.68 \text{ cm}^3 \text{ K mol}^{-1}$), that is, 9.62 (**9**), 10.19 (**11a**), 10.28 (**13**) and 9.47 (**15**) $\text{cm}^3 \text{ K mol}^{-1}$. This value stays constant until a sharp decrease occurs for the four complexes at approximately 60 K, reaching 0.30 (**9**), 1.02 (**11a**), 0.28 (**13**) and 0.94 (**15**) $\text{cm}^3 \text{ K mol}^{-1}$. This shows that in this family of compounds, the intramolecular magnetic coupling is dominated by anti-ferromagnetic interactions and that the ground state is diamagnetic. These observations are in great contrast to those previously made for the related complex $(\text{NMe}_4)_{10}[\text{Ni}_8(\text{cit})_6(\text{OH})_2(\text{H}_2\text{O})_2]$ (**16**, $\text{H}_4\text{cit} = \text{citric acid}$).^[12] The topology of the eight Ni^{II} centres within the $[\text{Ni}^{\text{II}}_8]$ core of this cluster is very similar to that within the $[\text{Ni}^{\text{II}}_8\text{M}^{\text{I}}_2]$ core of complexes **9** to **15** (Figure 9). However, the former complex exhibits pre-

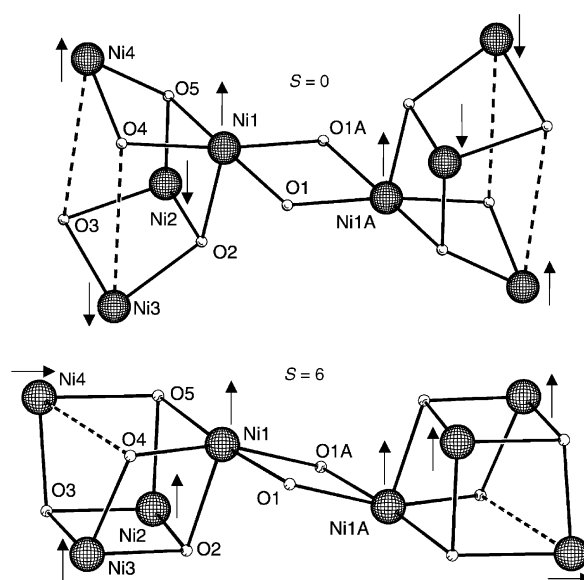


Figure 9. Core drawings of **9** (top representing complexes **9** to **15**) and **16** (bottom), showing the spin coupling scheme postulated to explain the ground state of the complexes (see text). The dashed lines are guides to the eye.

dominantly ferromagnetic interactions, yielding an $S_T = 6$ spin ground state. According to reported magneto-structural correlations performed on clusters with a $[\text{Ni}^{\text{II}}_4(\mu_3\text{-O})_4]$ core,^[13, 14] Ni-O-Ni angles smaller than 99° favour ferromagnetic interactions, whereas wider angles tend to give anti-ferromagnetic couplings. The main structural difference between the core of **16** and that of the $[\text{Ni}^{\text{II}}_8]$ clusters **9** to **15** is that in the former, the metals within the symmetry-related $[\text{Ni}^{\text{II}}_4]$ pseudo cubanes are bridged by three $\mu_3\text{-O}$ donors and only one $\mu_2\text{-O}$ moiety, instead of two $\mu_3\text{-O}$ and two $\mu_2\text{-O}$ atoms (see Figure 9). As a result, the average Ni-O-Ni angles in **16** are more acute, thus ferromagnetic interactions are more favoured. In Table 3 there is a comparison of the average Ni-O-Ni angles in complex **16** with those in **9** to **15** along with the type of interaction predicted by the above-mentioned correlations for the respective Ni-Ni pairs. The spin-coupling schemes shown in Figure 9 used to rationalise the $S = 6$ and

Table 3. Average core Ni-O-Ni angles [$^\circ$] for complexes **9**, **11**, **13**, **15** and **16**, and predicted coupling for each Ni-Ni pair.^[a]

	9	11	13 ^[b]	15 ^[b]	16 ^[c]
Ni1-O-Ni1A	96.11 (F)	96.81	97.43	94.64	95.35 (F)
				96.99	95.47
Ni1-O-Ni2	93.31 (F)	93.16	92.58	91.89	90.12 (F)
			93.03	92.48	
Ni1-O-Ni3	127.27 (AF)	127.79	128.77	129.02	97.26 (F)
			130.20	128.80	
Ni1-O-Ni4	93.32 (F)	94.83	95.8	95.82	122.55 (AF)
			94.65	95.09	
Ni2-O-Ni3	94.55 (F)	94.34	94.15	97.74	101.19 (AF)
			93.74	97.51	
Ni2-O-Ni4	127.11 (AF)	126.92	126.20	129.1	87.81 (F)
			126.55	128.62	
Ni3-O-Ni4	–	–	–	–	117.96 (AF)

[a] Predictions for complexes **11**, **13** and **15** are the same as for **9**. [b] Two entries correspond to the two independent molecules in the unit cell. [c] Data taken from supplementary material to ref. [12].

$S = 0$ ground states of **16** and **9** to **15**, respectively, agree with most of the predictions in Table 3. For **16**, the only contradiction is that of the Ni2–Ni3 coupling, predicted as anti-ferromagnetic whilst postulated ferromagnetic in the scheme. This can be explained by the presence of the ferromagnetic interactions Ni1–Ni2 and Ni1–Ni3, which force the spins of Ni1 and Ni3 to align. The spin frustration postulated for Ni4 in **16** is also caused by the presence of competing interactions. In complex **9**, the coupling Ni1–Ni2 is proposed to be opposite (AF) to that predicted (F), again forced by the coupling between pairs Ni2–Ni3 (F) and Ni2–Ni4 (AF).

Conclusion

In this report, we have demonstrated that by using the serendipitous approach, a large variety of interesting topologies can be made by introducing slight and sensible variations to a common reaction system. These changes come to mind through observation of the outcome of previous reactions. Thus, by modifying the nature of the alkali metal used in the synthesis, fourteen new $[\text{Ni}^{\text{II}}_x]$ clusters that have pivalate and pyrazolines as bridging ligands have been prepared and crystallographically characterised, displaying a large variety of structures. Saalfrank has previously shown^[15] that variation of alkali metal can control the nuclearity of metallocoronands by “templating” the formation of the metal wheel about monocations of different size. Here, variation of the alkali metal has a similar, but less easily rationalised effect. The preliminary magnetic characterisation shows that the family of compounds prepared during this study display primarily antiferromagnetic intramolecular magnetic exchange. A sensible rationalisation of the spin ground state of each complex can be made in the form of a spin-coupling scheme by inspection of the geometry and structural parameters. A detailed study is under way in order to establish the precise influence of the different structural and chemical factors on the magnetic properties of the various members of this large family. Expansion of this group of complexes by introducing cations of the alkaline-earth group instead of alkali metals is under investigation.

Experimental Section

Syntheses: All reagents were used as received unless indicated otherwise. The ligand Hppo (3-phenyl-3-pyrazolin-5-one) was prepared as published elsewhere.^[16] $[\text{Ni}_2(\text{H}_2\text{O})(\text{piv})_4(\text{Hpiv})_4]$ (**1**) was prepared according to a literature method.^[9]

3-Ethyl-3-pyrazolin-5-one (Hepo): A solution of 64% aqueous hydrazine (5.7 mL, 72 mmol) in ethanol (40 mL) was added to a stirred solution of ethyl propanoacetate (10.4 g, 72 mmol) in ethanol (40 mL), and the mixture was heated reflux for 3 hours. Upon cooling the solution to room temperature, a white precipitate of Hepo formed, which was collected by filtration. A second crop of the product was obtained from the filtrate after it had been left standing for two days at 5°C. The overall yield was 84%. ¹H NMR (CD_3OD): $\delta = 1.25$ (t, 3H; CH_3), 2.57 (q, 2H; CH_2); IR: $\tilde{\nu} = 1616$ vs, 1546 s, 1507 s, 1458 s, 1321 s, 1240 m, 1189 s, 1153 m, 1061 w, 1016 m, 990 m, 948 m, 880 m, 795 m, 756 s, 741 m, 615 w, 544 w, 529 m, 431 w, 417 cm^{-1} w; elemental analysis calcd (%) for $\text{C}_8\text{H}_{12}\text{N}_2\text{O}$ (112.13): C 53.56, H 7.19, N 24.98; found: C 53.72, H 7.19, N 24.87; EI: m/z : 112 $[M - \text{H}]$.

3-Trifluoromethyl-3-pyrazolin-5-one (Hfpo): A solution of 64% aqueous hydrazine (9.5 mL, 112 mmol) in ethanol (70 mL) was added to a stirred solution of ethyl trifluoroacetate (22.1 g, 112 mmol) in ethanol (70 mL), and the mixture was heated under reflux for 3 hours. The mixture was then cooled to room temperature and left undisturbed overnight. After this, the solvent was removed under reduced pressure, and a crude product was obtained, which was redissolved in EtOH. The solution was concentrated under reduced pressure until a crystalline solid started to precipitate. The mixture was left for a few hours at 5°C, and then the solid was collected by filtration and washed with cold diethyl ether. A second crop of the product was obtained from the filtrate after a few days. The overall yield was about 60%. IR: $\tilde{\nu} = 1604$ vs, 1506 s, 1420 s, 1253 vs, 1193 m, 1138 vs, 1094 s, 995 s, 777 s, 697 s, 659 w, 504 cm^{-1} w; elemental analysis calcd (%) for $\text{C}_8\text{H}_5\text{F}_3\text{N}_2\text{O}$ (152.08): C 31.59, H 1.99, N 18.42; found: C 31.72, H 1.83, N 18.43; EI: m/z : 152 $[M - \text{H}]$.

Complexes: General reaction: All complexes except **15** were prepared in a similar manner. A solution of complex $[\text{Ni}_2(\text{H}_2\text{O})(\text{piv})_4(\text{Hpiv})_4]$ (**1**, 600 mg, 0.63 mmol) in MeOH (20 mL) was mixed with a solution of the corresponding pyrazolinol ligand and base in MeOH (20 mL). The mixture was stirred overnight, and the solvent was removed under reduced pressure. The crude product, which consisted of a green powder or oil, was extracted with MeCN (20 mL) and filtered (except where indicated otherwise), and the filtrate was left undisturbed for a few days, after which crystals of the corresponding complex were collected by filtration.

$[\text{Ni}_4\text{Na}_4(\text{fpo})_4(\text{piv})_8(\text{Hpiv})_8]$ (2**):** Complex **2** was prepared as indicated above by using Hfpo (152 mg, 1.0 mmol) and a solution of NaOMe in MeOH (0.5 M, 2 mL, 1.0 mmol). In this case, the reaction crude was stirred with MeCN (20 mL), and the product was obtained as a precipitate and collected by filtration. Yield: 45%; elemental analysis calcd (%) for $\text{C}_{96}\text{H}_{160}\text{F}_{12}\text{N}_8\text{Na}_4\text{Ni}_4\text{O}_{36}$ (**2**, 2557.07): C 45.09, H 6.31, N 4.38; found: C 45.37, H 6.17, N 4.30.

$[\text{Ni}_4\text{Na}_4(\text{mpo})_4(\text{piv})_8(\text{Hpiv})_8]$ (3**):** Complex **3** was prepared by using Hmpo (98 mg, 1.0 mmol) and a methanolic solution of NaOMe (0.5 M, 2 mL, 1.0 mmol). After the solvent had been removed, the crude was extracted with MeCN (20 mL) and filtered. The product was obtained as green crystals from the filtrate after a few days. Yield: 42%; elemental analysis calcd (%) for $\text{C}_{86}\text{H}_{152}\text{N}_8\text{Na}_4\text{Ni}_4\text{O}_{32}$ (**3**, 2136.92): C 48.34, H 7.17, N 5.24; found: C 48.20, H 7.28, N 5.16.

$[\text{Ni}_4\text{Na}_4(\text{epo})_4(\text{piv})_8(\text{Hpiv})_8]$ (4**):** For the preparation of **4**, Hepo (112 mg, 1.0 mmol) and a methanolic solution of NaOMe (0.5 M, 2 mL, 1.0 mmol) were used. After evaporation of the solvent, the crude was stirred with MeCN, and the product was collected by filtration. A second crop of the product was collected from the filtrate in crystalline form after a few days. Total yield: 51%; elemental analysis calcd (%) for $\text{C}_{88}\text{H}_{150}\text{N}_8\text{Na}_4\text{Ni}_4\text{O}_{30}$ (**4**, 2090.90): C 48.83, H 7.23, N 5.36; found: C 49.10, H 7.40, N 5.29.

$[\text{Ni}_5\text{Na}_4(\text{OH})_2(\text{mpo})_4(\text{piv})_8(\text{Hpiv})_2(\text{MeCN})_2]$ (5**):** In the preparation of **5**, the basic solution of ligand contained Hmpo (124 mg, 1.26 mmol) and a methanolic solution of NaOMe (0.5 M, 5.04 mL, 2.52 mmol). The crude from the reaction was stirred with MeCN, and the mixture was filtered. A large amount of green solid was discarded, and crystals of the product were obtained from the filtrate after a few days. Yield: 19%. The complex was found to gain one molecule of water upon exposure to air. Elemental analysis calcd (%) for $\text{C}_{70}\text{H}_{120}\text{N}_{10}\text{Na}_4\text{Ni}_5\text{O}_{26} \cdot 2\text{H}_2\text{O}$ (**5**·2H₂O, 1921.21): C 43.76, H 6.40, N 7.29; found: C 43.46, H 6.44, N 7.23.

$[\text{Ni}_5\text{Na}_4(\text{OH})_2(\text{epo})_4(\text{piv})_8(\text{MeCN})_4]$ (6**):** In the preparation of **6**, the mixture of ligand and base consisted of Hepo (142 mg, 1.27 mmol) and NaOMe (416 mg, 7.7 mmol). From the filtrate of MeCN after extraction, crystals of the product were obtained in 13% yield. Microanalysis showed that, upon exposure to air, MeCN was partially substituted by H₂O to form $[\text{Ni}_5\text{Na}_4(\text{OH})_2(\text{epo})_4(\text{piv})_8(\text{H}_2\text{O})_2(\text{MeCN})_2]$ (**6a**). Elemental analysis calcd (%) for $\text{C}_{64}\text{H}_{112}\text{N}_{10}\text{Na}_4\text{Ni}_5\text{O}_{24}$ (**6a**, 1791.07): C 42.92, H 6.30, N 7.82; found: C 43.01, H 6.28, N 8.01.

$[\text{Ni}_5\text{Na}_4(\text{OH})_2(\text{ppo})_4(\text{piv})_8(\text{Hpiv})_2(\text{EtOAc})_2]$ (7**):** For the preparation of **7**, Hppo (203 mg, 1.27 mmol) and a methanolic solution of NaOMe (0.5 M, 5.04 mL, 2.52 mmol) were used. The extraction in this case was performed with AcOEt, and from this mixture a white solid was removed by filtration. Crystals of the product were obtained from the filtrate after a few days in 12% yield. Microanalysis showed that upon exposure to air the solvate molecules were replaced by H₂O to form $[\text{Ni}_5\text{Na}_4(\text{OH})_2(\text{ppo})_4(\text{piv})_8$

(H piv)₂(H₂O)₂ (**7a**). Elemental analysis calcd (%) for C₈₆H₁₂₆N₈Na₄Ni₅O₂₈ (**7a**, 2105.41): C 49.06, H 6.03, N 5.32; found: C 49.13, H 5.97, N 4.96.

[Ni₅Li₆(OH)₂(fpo)₂(piv)₁₂(Hpiv)₄] (**8**): Complex **8** was synthesised by using Hfpo (192 mg, 1.26 mmol) and a methanolic solution of LiOMe in MeOH (1M, 1.26 mL, 1.26 mmol). Extraction of the crude with MeCN produced crystals of the product after two weeks in 50% yield. Elemental analysis calcd (%) for C₈₈H₁₅₄N₄Li₆Ni₅O₃₆ (**8**, 2293.30): C 46.09, H 6.77, N 2.44; found: C 46.11, H 6.65, N 2.59.

[Ni₅K₂(OH)₄(ppo)₄(piv)₁₀(Hppo)₂(Hpiv)₂(MeCN)₂] (**9**): Complex **9** was obtained by using Hppo (151 mg, 0.95 mmol) and an ethanolic solution of KOEt (2.55 M, 124 μL, 0.32 mmol). Crystals of the product were obtained after a few days from the MeCN extract in 9% yield. Elemental analysis calcd (%) for C₁₁₈H₁₆₆N₁₄K₂Ni₅O₃₆ (**9**, 2888.43): C 49.07, H 5.79, N 6.79; found: C 48.91, H 5.83, N 6.68.

[Ni₅K₂(OH)₄(epo)₄(piv)₁₀(Hepo)₄(MeCN)₂] (**10**): For the preparation of **10**, the basic solution of ligand contained Hepo (141 mg, 1.26 mmol) and an ethanolic solution of KOEt (2.55 M, 124 μL, 0.32 mmol). Crystals of the complex were obtained from the MeCN extract after one week in 6% yield. Microanalysis showed that the compound desolvated upon exposure to air to yield [Ni₅K₂(OH)₄(epo)₄(piv)₁₀(Hepo)₄] (**10a**). Elemental analysis calcd (%) for C₉₀H₁₅₄N₁₆K₂Ni₅O₃₂ (**10a**, 2520.03): C 42.90, H 6.16, N 8.89; found: C 43.29, H 5.87, N 8.42.

[Ni₅Rb₂(OH)₄(ppo)₄(piv)₁₀(Hppo)₂(Hpiv)₂(MeCN)₂] (**11**): In the preparation of **11**, Hppo (151 mg, 0.94 mmol) and an aqueous solution of RbOH (8.5 M, 37 μL, 0.31 mmol) were employed. Within a few days, crystals of the complex were obtained in 16% yield from the MeCN filtrate. Microanalysis showed that upon exposure to air the solvate molecules were replaced by H₂O to form [Ni₅Rb₂(OH)₄(ppo)₄(piv)₁₀(Hppo)₂(Hpiv)₂(H₂O)₂] (**11a**). Elemental analysis calcd (%) for C₁₁₄H₁₆₂N₁₂Rb₂Ni₅O₃₆ (**11a**, 2917.08): C 46.94, H 5.60, N 5.76; found: C 46.58, H 5.46, N 5.84.

[Ni₅Rb₂(OH)₄(epo)₄(piv)₁₀(Hepo)₄(MeCN)₂] (**12**): In the synthesis of **12**, the mixture of ligand and base was formed from Hepo (141 mg, 1.26 mmol) and an aqueous solution of RbOH (8.5 M, 37 μL, 0.31 mmol). Crystals of the complex were obtained, as above, in 8% yield. Microanalysis showed that the compound desolvated upon exposure to air to yield [Ni₅Rb₂(OH)₄(epo)₄(piv)₁₀(Hepo)₄] (**12a**). Elemental analysis calcd (%) for C₉₀H₁₅₄N₁₆Rb₂Ni₅O₃₂ (**12a**, 2612.77): C 41.37, H 5.94, N 8.58; found: C 41.61, H 6.02, N 8.02.

[Ni₅Cs₂(OH)₄(ppo)₄(piv)₁₀(Hppo)₂(Hpiv)₂(MeCN)₂] (**13**): In the preparation of **13**, Hppo (151 mg, 0.94 mmol) and an aqueous solution of CsOH (5.74 M, 55 μL, 0.31 mmol) were used. The desired product was obtained as a crystalline solid from the MeCN extract after three days in 15% yield. Elemental analysis calcd (%) for C₁₁₈H₁₆₄N₁₄Cs₂Ni₅O₃₄ (**13**, 3058.03): C 46.35, H 5.41, N 6.41; found: C 46.74, H 5.20, N 6.67.

[Ni₅Cs₂(OH)₄(epo)₄(piv)₁₀(Hepo)₂(Hpiv)₂(MeCN)₂] (**14**): The basic ligand solution in the reaction to form **14** was composed of Hepo (141 mg, 1.26 mmol) and an aqueous solution of CsOH (5.74 M, 55 μL, 0.31 mmol). Crystals of the product were collected from the MeCN extract in 17% yield after four weeks. Microanalysis showed that the compound desolvated upon exposure to air to yield [Ni₅Cs₂(OH)₄(epo)₄(piv)₁₀(Hepo)₂(Hpiv)₂] (**14a**). Elemental analysis calcd (%) for C₉₀H₁₆₀N₁₂Rb₂Ni₅O₃₄ (**14a**, 2689.67): C 40.19, H 6.00, N 6.25; found: C 40.05, H 6.00, N 6.50.

[Ni₈(OH)₄(mpo)₂(PhCH₂CO₂)₁₀(Hmpo)₈] (**15**): A mixture containing Ni(NO₃)₂·4H₂O (2.91 g, 0.01 mol), Na(PhCH₂CO₂) (1.76 g, 0.01 mol) and Na(mpo) (1.38 g, 0.01 mol) in MeOH (100 mL) was stirred overnight. Evaporation of the solvent led to a crude material, which was extracted with EtOAc and filtered. The filtrate was left undisturbed for a few days and slowly produced crystals of **15** to 26% yield. Elemental analysis calcd (%) for C₁₂₀H₁₂₆N₂₀Ni₈O₃₄ (**15**, 2861.95): C 50.36, H 4.44, N 9.79; found: C 50.00, H 4.66, N 9.57.

X-ray crystallography: All complexes presented in this work have been characterised by X-ray diffraction; however, crystallographic details are given only for the representative complexes [Ni₄Na₄(fpo)₄(piv)₈(Hpiv)₈] (**2**), [Ni₅Na₄(OH)₂(mpo)₄(piv)₈(Hpiv)₂(MeCN)₂] (**5**), [Ni₅Li₆(OH)₂(fpo)₂(piv)₁₂(Hpiv)₄] (**8**), [Ni₅K₂(OH)₄(ppo)₄(piv)₁₀(Hppo)₂(Hpiv)₂(MeCN)₂] (**9**), [Ni₅Rb₂(OH)₄(ppo)₄(piv)₁₀(Hppo)₂(Hpiv)₂(MeCN)₂] (**11**), [Ni₅Cs₂(OH)₄(ppo)₄(piv)₁₀(Hppo)₂(Hpiv)₂(MeCN)₂] (**13**) and [Ni₈(OH)₄(mpo)₂(PhCH₂CO₂)₁₀(Hmpo)₈] (**15**). Data were collected on a Bruker SMARTAPEX CCD diffractometer (MoK_α, λ = 0.71073 Å) (**2**, **5**, **8**, **9**, **11** and **13**) or a Bruker SMART 1 K CCD diffractometer (synchrotron,

λ = 0.6869 Å) (**15**). The selected crystals were mounted within a plastic cryoloop (**2**, **5**, **8**, **9**, **11** and **13**) or on the end of a piece of glass wool (**15**) with Flombin oil and placed in the cold flow produced with an Oxford Cryosystems 700 Series Cryostream cooler (100 K, **2**, **5**, **8**, **9**, **11** and **13**) or an Oxford Cryosystems 600 series cryostream cooler (150 K, **15**). Complete hemispheres of data were collected by using ω scans (0.3° (**2**, **5** and **9**) or 0.2° (**15**); 40 (**2** and **9**), 30 (**11**), 20 (**8**) 10 (**5** and **13**) or 1 (**15**) seconds per frame). Integrated intensities were obtained with SAINT +^[17] and (for **2**, **5**, **13** and **15**) they were corrected for absorption by using SADABS.^[17] No absorption correction was made for compounds **8**, **9** and **11**. Structure solution and refinement were performed with the SHELXTL package.^[17] All the structures were solved by direct methods and completed by iterative cycles of ΔF syntheses and full-matrix least-squares refinement against F². The numbers of parameters used were 379, no restraints (**2**), 581, no restraints (**5**), 676, 18 restraints (**8**), 741, 36 restraints (**9**), 781, 72 restraints (**11**), 1722, no restraints (**13**) and 1940, 714 restraints (**15**).

CCDC-198089 (**2**), 198091 (**9**), 198092 (**15**), 203901 (**8**), 205386 (**13**) and 205387 (**11**) contain the supplementary crystallographic data for this paper. These data can be obtained free of charge via www.ccdc.cam.ac.uk/conts/retrieving.html (or from the Cambridge Crystallographic Data Centre, 12 Union Road, Cambridge CB2 1EZ, UK; fax: (+44) 1223-336033; or deposit@ccdc.cam.ac.uk).

Physical measurements: FTIR spectra were collected on a Perkin Elmer Spectrum RXI spectrometer. Electronic ionisation mass spectrometry was performed with a Hewlett–Packard 5890 Series II gas chromatograph coupled to a Fisons Instruments VG TRIO spectrometer. 300 MHz ¹H NMR spectra were measured on a Varian Unity Inova 300 instrument. Elemental analysis was performed in house with a Carlo Erba Instruments CHNS-O EA-1108 elemental analyser. Field-cooled measurements of the magnetisation of smoothly powdered microcrystalline samples of **4** (28.3 mg), **7a** (21.5 mg), **8** (42.3 mg), **9** (27.5 mg), **11a** (25.1 mg), **13** (40.7 mg) and **15** (45.0 mg) were performed in the range 300–1.8 K with a Quantum Design MPMS-7XL SQUID magnetometer with an applied field of 1 or 10 kG. Corrections for diamagnetic contributions to the magnetic susceptibility were performed by using Pascal's constants.

Acknowledgement

This work was supported by the EPSRC (UK), INTAS (00-172), The Royal Society, the CNRS et the Conseil Général d'Aquitaine.

- [1] J. Rojo, F. J. Romero-Salguero, J. M. Lehn, G. Baum, D. Fenske, *Eur. J. Inorg. Chem.* **1999**, 1421.
- [2] E. Breuning, U. Ziener, J. M. Lehn, E. Wegelius, K. Rissanen, *Eur. J. Inorg. Chem.* **2001**, 1515.
- [3] R. W. Saalfrank, U. Reimann, M. Goritz, F. Hampel, A. Scheurer, F. W. Heinemann, M. Buschel, J. Daub, V. Schunemann, A. X. Trautwein, *Chem. Eur. J.* **2002**, *8*, 3614.
- [4] R. W. Saalfrank, H. Glaser, B. Demleitner, F. Hampel, M. M. Chowdhry, V. Schunemann, A. X. Trautwein, G. B. M. Vaughan, R. Yeh, A. V. Davis, K. N. Raymond, *Chem. Eur. J.* **2002**, *8*, 493.
- [5] M. Fujita, K. Umamoto, M. Yoshizawa, N. Fujita, T. Kusukawa, K. Biradha, *Chem. Commun.* **2001**, 509.
- [6] R. E. P. Winpenny, *J. Chem. Soc. Dalton Trans.* **2002**, 1.
- [7] A. Müller, P. Kogerler, *Coord. Chem. Rev.* **1999**, *182*, 3.
- [8] A. Müller, P. Kogerler, A. W. M. Dress, *Coord. Chem. Rev.* **2001**, *222*, 193.
- [9] H. Andres, G. Chaboussant, H.-U. Güdel, E. J. L. McInnes, A. Parkin, S. Parsons, G. Rajaraman, A. A. Smith, G. A. Timco, R. E. P. Winpenny, unpublished results.
- [10] Harris notation describes the binding mode as [X₁Y₂Y₃...Y_n], in which X is the overall number of metals bound by the whole ligand, and each value of Y refers to the number of metal atoms attached to the different donor atoms. Therefore for fpo, there will be two values for Y. The ordering of Y is listed by the Cahn–Ingold–Prelog priority rules, hence O before N. See: R. A. Coxall, S. G. Harris, D. K. Henderson, S. Parsons, P. A. Tasker, R. E. P. Winpenny, *J. Chem. Soc. Dalton Trans.* **2000**, 2349.

- [11] J. Krzystek, J. H. Park, M. W. Meisel, M. A. Hitchman, H. Strate-meier, L. C. Brunel, J. Telser, *Inorg. Chem.* **2002**, *41*, 4478.
- [12] M. Murrie, D. Biner, H. Stoeckli-Evans, H. U. Güdel, *Chem. Commun.* **2003**, 230.
- [13] J. M. Clemente-Juan, B. Chansou, B. Donnadieu, J. P. Tuchagues, *Inorg. Chem.* **2000**, *39*, 5515.
- [14] M. A. Halcrow, J. S. Sun, J. C. Huffman, G. Christou, *Inorg. Chem.* **1995**, *34*, 4167.
- [15] R. W. Saalfrank, I. Bernt, E. Uller, F. Hampel, *Angew. Chem.* **1997**, *109*, 2596; *Angew. Chem. Int. Ed. Engl.* **1997**, *36*, 2482.
- [16] G. Aromí, A. Bell, S. J. Teat, A. G. Whittaker, R. E. P. Winpenny, *Chem. Commun.* **2002**, 1896.
- [17] *SHELX-PC Package*. Bruker Analytical X-ray Systems: Madison, WI, **1998**.

Received: March 11, 2003 [F4939]